

# Evaluation of Machine Learning Techniques for the Nd: YAG Laser & TIG Welded Stainless Steel 304

**Varun Kumar A**

Assistant Professor (Sr. Gr.)  
B.S. Abdur Rahman Crescent Institute of  
Science & Technology  
Department of Mechanical Engineering  
India

**Pradeep Krishna R**

Design Engineer Trainee  
Aptiv Connection Systems  
India

**Masood Fakouri Hasanabadi**

Assistant Professor  
Iranian Research Organization for Science  
and Technology  
Department of Advanced Materials and  
Renewable Energy  
India

**Sathickbasha K**

Assistant Professor (Sr. Gr.)  
B.S. Abdur Rahman Crescent Institute of  
Science & Technology  
Department of Mechanical Engineering  
India

*Nd: YAG Laser and Tungsten Inert Gas (TIG) welding processes are the most promising joining techniques used for stainless steel (SS) alloys due to their significant weld characteristics. In this study, the effect of two process parameters (weld power and travel speed) on the mechanical properties (ultimate tensile strength and microhardness) of the weldment is investigated. Two different machine learning techniques, namely Adaptive Neuro-Fuzzy Inference System (ANFIS) and Unified Convolutional Neural Network (UCNN) are also evaluated for prediction of mechanical properties and defect detection through the image processing technique, respectively. A correlation has been performed between these two machine learning approaches with the experimental values. The training data sets are developed for the machine learning techniques, and the obtained results of (ANFIS) and (UCNN) models are related to the actual experimental values. The output of both developed models (ANFIS & UCNN) showed a good agreement with the actual experimental test results. The predicted tensile and microhardness values from the (ANFIS) model were found to greatly agree with the Peak Signal-to-Noise Ratio (PSNR) values from the (UCNN) model. However, owing to the increase in the applications of welding processes in industries, the utilization of machine learning techniques would be more efficient when compared with the other traditional methods that are being adopted.*

**Keywords:** Stainless Steel 304, Nd: YAG Laser Welding, TIG Welding, Mechanical Properties, ANFIS, UCNN).

## 1. INTRODUCTION

Austenitic Stainless Steels (ASS) are being widely used in various applications (structural materials, valves, vessels, etc.) due to their promising and unique characteristics such as enhanced toughness, better temperature resistance, and good resistance towards corrosion when compared with other grades of steels. Owing to their superior material properties, their utilization in different applications has become unavoidable recently. However, the superior properties exhibited in an ASS will be affected by any joining process due to the changes in grain boundaries/structures, porosity, solidification cracking, material loss through vaporization, etc. [1, 2]. Therefore, to retain the properties of the alloy, it is necessary to select a suitable welding process and optimal process parameters. In general, it is well-known that the welding process has been widely used to fabricate steel joints for either a similar or dissimilar category. Though there are different welding processes available for the fabrication of steel joints, laser beam welding (LBW) and tungsten inert gas (TIG) welding have been found as promising techniques. The LBW has been increased in its adoption in the industries due to its high

energy beam density, which helps in the quick fabrication of the joints [3, 4]. Further, this process carries some significant properties such as a narrow heat-affected zone (HAZ), high depth of penetration, and high welding speed [5]. These unique properties/characteristics of LBW make them important in the industrial sectors. Similarly, among the different conventional welding processes, the gas tungsten arc welding (GTAW) process is much preferred for its good weld quality [6]. Research works have reported that the process parameters had a significant influence on the material property of the weldments [7–11]. Pertaining to the concern on the process parameters influence over the material property of weldment, the need for the optimization of process parameters has increased rapidly to meet the industrial requirements. Since the welding process involves complex factors such as the formation of intermetallic, diffusion of atoms and elements, solidification of the melt pool, etc. However, these issues can certainly be addressed efficiently with the proper utilization of the process parameters in a welding process. Nowadays, a variety of non-linear methods are being adopted, such as the Taguchi method [12–15], the response surface method [16–20], the artificial neural network (ANN) [21–25], genetic algorithm [26, 27], and the particle swarm optimization techniques [28–30] have been predominantly used to find the relation between the process parameters and their associated desired outputs to represent the optimal weldment in all aspects.

Received: September 2023, Accepted: December 2023

Correspondence to: Dr Sathickbasha K  
Department of Mechanical Engineering,  
BSACIST, Vandalur, Chennai 600 048, India.

E-mail: sathick.basha@crescent.education

doi: 10.5937/fme2401090K

© Faculty of Mechanical Engineering, Belgrade. All rights reserved

FME Transactions (2024) 52, 90-102 90

Wide research works are performed with traditional optimization techniques such as Taguchi orthogonal array and grey relational analysis for predicting the optimal process parameters. However, due to the rapid growth in manufacturing firms, machine learning techniques play a major role due to their reduced time factor in determining the suitable working parameter in a process. Owing to the above requirements in the industries for the prediction of optimal weldment, the Adaptive Network-based Fuzzy Inference System (ANFIS) and Unified Convolutional Neural Network (UCNN) significantly influenced the enhancement of accuracy level in the prediction of output values to a greater extent. ANFIS is a predictive model that utilizes both the neural network and fuzzy logic to map the inputs and outputs [31]. The ANFIS model had been very predominantly used in the prediction of the tensile strength of the weldments, and these ANFIS models had been compared with other methods Artificial Neural Network (ANN), Taguchi, ANOVA, RSM [32–35]. The Convolutional Neural Network (CNN) is being widely used as a technique for the prediction of weld quality in terms of porosity and defects that occur in a welding process [36–40], the CNN uses training data sets for the prediction of the defects. However, the weld defects were also determined using image processing methodology, which implements methods like the Peak Signal-to-Noise Ratio (PSNR) and noise filters for the required output [41–45]. The Adaptive Median Filters (AMF) are also being used for the prediction of defects, which proved that the AMF could be used for the better determination of the defects in a weld sample [46]. Though research works are performed by using other different machine learning techniques, with varying models that are available strong literature shows that the ANFIS and UCNN models had put significant effect on the different welding processes. The UCNN approach specifically reduces a lot of time factor in detecting the weld defects which normally takes more pre-processing and post-processing work on a fabricated sample in conventional NDT techniques. Thus, comparing these two techniques is a major novelty of the current study.

Nevertheless, no evident research works reported comparing the two different machine learning techniques (ANFIS and UCNN). However, the adoption of these two machine learning techniques will significantly impact the optimization approach and other conventional techniques that are used for defect detection. The mass production industries will benefit highly benefitted with the adoption of these techniques which greatly reduce the time factor that is being spent in the current practice. Therefore, in this present study, a comparison of the above two different machine learning techniques was attempted. We have made a correlation between the predicted mechanical properties of the weldment through the ANFIS model to that of (PSNR) values obtained for the corresponding optical microstructures through the image processing technique. The theoretical data derived from the ANFIS and UCNN models are compared with the experimental values from our previous work [47]. Our previous research is to achieve and predict a sound joint between two similar (SS 304) alloys through two different joining processes

Nd: YAG Laser Welding and (TIG) welding. The training data sets for the (ANFIS) model are developed based on the process parameters (power, travel speed, and hole depth). The image processing for the defect detection of the samples is performed using four different median filters (Adaptive Median Filter, 2D Hybrid Median Filter, 2D Adaptive Log Gabor, 2D Adaptive Anisotropic Bilateral Diffusion Filter). The images for the image processing technique were procured from our previous study pertaining to the (LW) and (TIG) welding of (SS 304) [48].

## 2. MACHINE LEARNING METHODS

### 2.1 Artificial Neural Network (ANN)

The Artificial Neural Network (ANN) is a simplified version of the Biological Neural Network (BNN). The neurons are an interconnected system of the nervous system which consists of (computer input signals, transportation of signals at high speed, storage of information, perception, automatic training, and modeling). In ANN the inputs (X) will be carrying a weight percentage (W), which will be assembled in the summation unit in the form of  $[(X_1 \times W_1) + \dots + (X_n \times W_n)]$ . From the summation unit, the received signals will be forwarded to the threshold unit. Here if the received signals are greater than the threshold limit that will be further passed on to the output, the signals that are less than the threshold unit will not be further processed to the output. The threshold unit is also termed a transfer function denoted ( $\Phi$ ). The term ( $\Phi$ ) is said to be a step function which is also defined as the Heaviside function. These transfer functions in the ANN can be further classified as a hard-limit transfer function, linear transfer function, and sigmoid transfer function. The above-mentioned transfer functions are very popular and widely adopted in the ANN. Figure 1 shows the schematic representation of the ANN model, which consists of three layers. The input layer is composed of the used input parameters, the processed input parameters are kept and performed in the hidden layer, and the optimized output is determined at the third layer. The ANN has superior mapping capabilities when compared with the other traditional methods; therefore, the ANN is adopted in situations where the inclusion of a mathematical model is complex. The very first ANN model was adopted for the GTAW process [49]. An improved ANN and neural network model were performed in the prediction and selection of different welding processes [50 - 53]. The ANN can be performed with different algorithms depending on the applications. The well-familiar algorithms are the back-propagation, counter-propagation, and genetic algorithms. The above-mentioned are very widely adopted algorithms pertaining to the ANN model due to their well-exhibited characteristics compared to the other algorithms that exist. However, the material joining process is a factor that highly depends on the process parameter irrelevant to the type of process that is being adopted. Few research studies have reported how the process parameters impact the property of a bonding [54]. Based on the ambiance of the weld atmosphere

(noise level) and emission of fumes from the process performed to improve the joint characteristics in a safe manner [55, 56]. The weld quality has been determined using various methodologies to have a better bonding between the alloys [57], in this work the faults and defects are represented in a feasible approach. The major difficulty in a laser welding process is the control of distortion in the joining process, [58] has reported work on the distortion control by adopting the TAGUCHI methodology for a flexible approach to usage.

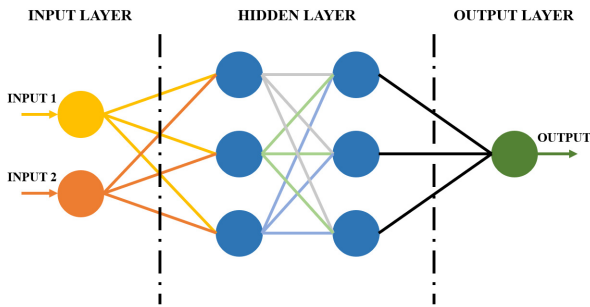


Figure 1. Schematic representation of ANN with two input variables [32]

## 2.2 Adaptive Neuro-Fuzzy Inference System (ANFIS)

Takagi and Sugeno's approach is represented as (ANFIS), the model was developed in early 1993 later it has obtained a wide scope in various applications for their efficiency and accuracy when compared with the other existing neural network models. In the (ANFIS) model, the input is considered to be a linear distribution, for much more accuracy a non-linear distribution can be utilized in the developed model, whereas the output is always a function of inputs. The inputs are considered to be a membership distribution function which is distinguished by three linguistic terms. If we consider two inputs ( $I_1^*$  and  $I_2^*$ ) during the training and model development, we will be varying the ( $d_1$  and  $d_2$  – represent the length of the distribution function) for obtaining a modified distribution in the given inputs. In general, the ANFIS model consists of 6 layers (Layer 1 – Inputs, Layer 2 – Fuzzification, Layer 3 – Firing strength values, Layer 4 – Normalized firing strength values, Layer 5 – Outputs calculated as the product of normalized firing strength values, and Layer 6 – Overall output for the trained and developed model) each layer will be having a significant role in deciding the training and model development. The schematic representation of the ANFIS architecture can be referred to in Figure 2. It can be observed from Figure 2, there are notations in terms of circles and squares.

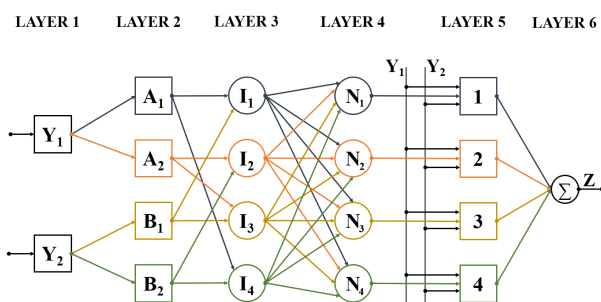


Figure 2. ANFIS Architecture [48]

The squared variables define that further optimization can achieve much more enhanced accuracy in the trained and developed model. The further optimization can be of error minimization algorithms with the assistance of input variables coefficients ( $a_i$ ,  $b_i$ , and  $c_i$ ). If we adopt a Genetic Algorithm for further optimization, it is termed as ANFIS model. However, the ANFIS model is the well-defined solution for the theoretical prediction of the values.

## 2.3 Convolutional Neural Network (CNN)

The Convolutional Neural Network (CNN) is said to be a special case of the existing Artificial Neural Network (ANN). The CNN uses the images as the inputs, whereas the ANN uses the inputs as vector values or labels. However, the complexity that exists in the ANN methods is easily eliminated with the adoption of the CNN, such as the sparse between the layers and weight sharing are possible in the CNN. The sparse and the weight sharing had a promising effect on the reduction of the matrix sizes to a greater extent, thus we could be able to achieve the desired output with minimal connections and layers. Due to these factors, CNN played determining roles in image recognition, object detection, semantic segmentation, and medical image analysis. The images are typically recognized with the adoption of filters or kernels. The specific filter or kernel can be utilized in the image recognition process, for example, a curve in the image with a particular orientation of angle can be predicted with the same filter or kernel. Generally, the images are said to be in the range of 0 to 255 pixels, which is mentioned as an 8-bit image. The input images can be of grayscale or RGB image, where the RGB image is composed of 3 channels. The inputs are derived from the pixels along the horizontal and the vertical axis as ( $n_x$  and  $n_y$ ). Therefore, in the case of the grayscale images, the input will be of ( $n_x \times n_y$ ), and in the case of RGB images, the input will be of ( $n_x \times n_y \times 3$ ). The obtained output volume from the CNN is also to be termed a feature map or activation map, the size control of the feature or activation map is easily controlled when compared with the other traditional methods.

## 2.4 Adaptive Filters (AF)

Generally speaking, the images observed in a process will tend to degrade due to various environmental facts, equipment errors, etc. Therefore, there is always a large scope required in the enhancement of procured or observed images from the experiments. In this scenario, the Adaptive Filters (AF) play a major role in the restoration of the images that are said to be degraded due to different factors. These AF will be helpful in the enhancement of the observed images in an efficient manner. Similarly, the defects in the images are also found to be well-identified through these filters to a greater extent when compared with other techniques. The variations in the degraded images can be validated with the Peak Signal-to-Noise Ratio (PSNR) values. The validation of the defects through PSNR values is highly commendable and recommended in the welding

processes; these AF techniques have overcome the challenges that exist in the Non-Destructive Testing (NDT) methods. Different types of AF techniques are available, and depending on the higher PSNR values the optimal filter can be selected for the better detection of defects in a welding process. This restoration of the procured images through the image processing technique falls in the Unified Convolutional Neural Network UCNN model.

### 3. EXPERIMENTS AND RESULTS

#### 3.1 Experiments

The base metal used in this study is (SS 304) which is often used in wide applications due to its superior material properties, as discussed in the earlier section. The plate dimensions are (300 × 150 × 2) mm, which are machined with laser cutting to maintain accurate dimensions and have a good surface finish. Two different welding processes are adopted to fabricate joints between the metals, namely (the TIG Welding process and the Nd: YAG Laser Welding process). The need for two different joining processes is to identify the suitable process for the (SS 304), owing to their tremendous requirement in different applications. A total of two samples are fabricated through the TIG and Nd: YAG Laser welding process. In our previous work [47] we have related the material properties of the weldments with their free vibrational characteristics. In this study, the welding power and travel speed are considered key process parameters for developing the model using a machine-learning approach.

#### 3.2 Experimental results

It is reported and discussed in our previous study [47], that the refinement in the grain boundaries will have a significant effect on the enhancement of material properties (tensile and microhardness). However, this refinement in the grain can be achieved with the proper selection of the joining process, process parameters, and the addition of external powder particles. The obtained microstructures from the experiments are depicted in Figure 3 (A-D). Figure 3 (A-D) describes the metallurgical aspects of the laser and TIG welded joints. It is reported in our previous investigation [47], that refinement of grains is achieved with the addition of powders with the base metal, and also the welding process used will play a major role in the metallurgical happenings across the weld pool region.

**Table 1. Process parameters [47]**

SI. No	Weld technique used	Power	Travel speed (mm/s)	Hole depth (mm)
1	Nd: YAG	190 (W)	5	3
2	TIG	180 (A)	8	3

Due to these refinements in the grain structures, the enhancement in the tensile and microhardness are predicted. The achieved test result values of the tensile

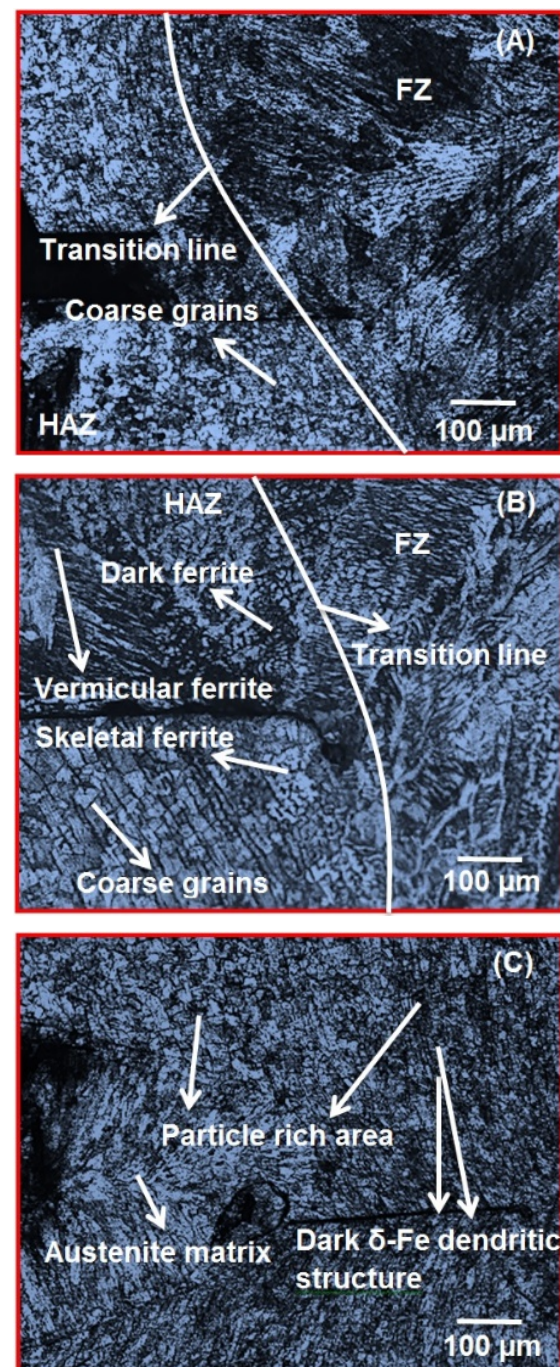
test and the microhardness are reported in Tables 2 and 3. In the present investigation, we have utilized the (tensile and microhardness) values for the (ANFIS) model, and the optical microstructures observed in the Heat-Affected Zone (HAZ) and Fusion Zone (FZ) are considered for the (UCNN) model.

**Table 2. Ultimate tensile strength values [47]**

SI. No	Sample	UTS (MPa)
1	Base metal	≈ 501
2	Nd: YAG Laser welded sample	≈ 578
3	TIG welded sample	≈ 532

**Table 3. Microhardness values [47]**

SI. No	Sample	Hv
1	Base metal	≈ 162
2	Nd: YAG Laser welded sample	≈ 271
3	TIG welded sample	≈ 221



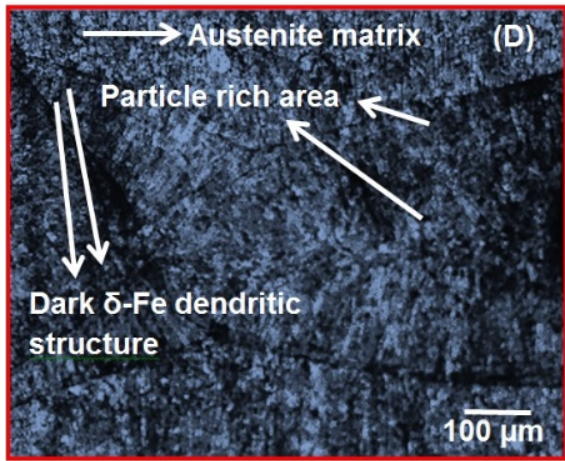


Figure 3 (A-D): (A) HAZ – Laser welded joint, (B) HAZ – TIG welded joint, (C) FZ – Laser welded joint, and (D) FZ – TIG welded joint [47]

#### 4. ANFIS MODELLING AND VALIDATION

##### 4.1 Input variable for ANFIS model

To obtain the ANFIS model a total of 3 input variables are used in this work. The study was made with the variables (power, travel speed, and depth hole ratio). The adopted process parameters in this study are listed in Table 1 for two different welding processes. Tables 2 and 3 reveal that the welding process and the process parameters used had a significant effect on the tensile properties and microhardness values. From the test results, the base metal of (SS 304) showed lower tensile and microhardness values when compared with the samples fabricated via Nd: YAG Laser welding and TIG welding process. Comparing the tensile and microhardness values of Nd: YAG Laser welding and the TIG welding process, the laser-welded samples showed promising improvement in the values of mechanical properties. However, relating the process parameters with the material properties is always quite complex and tedious with the traditional methods that exist. This made a large scope for adopting the statistical learning model (ANFIS). ANFIS can be predominantly used for the development of predictive values.

##### 4.2 ANFIS model development for the prediction of mechanical properties

ANFIS model is developed for the samples fabricated for the process parameters listed in Table 1. The models are developed to predict the tensile and microhardness values. The ANFIS model is a unique and productive methodology that can be widely used for the theoretical prediction of values such as tensile strength and hardness. ANFIS model is part of the artificial neural networks (ANN), though different techniques exist in the (ANN). ANFIS models were widely utilized in various applications due to their flexibility in developing the trial model for the theoretical prediction of values. Figure 4 shows the schematic representation of the ANFIS model developed for the samples fabricated with different process parameters. Tables 4 and 6 depict the (RMSE & MAPE) values for different membership functions, it can be observed in the Tables that the

Gauss membership functions possess with least error values when compared with the other membership functions. The achieved experimental test result values and the predicted values of tensile and microhardness are reported in Tables 5 and 7. In this experimental trial, a minimum number of samples was fabricated, therefore, to develop the ANFIS model few other process parameters are assumed for better validation and measurement of the error. It can be depicted from the Tables that the test result values and the predicted values have fewer errors for both the joining processes. Therefore, it can be considered that the ANFIS model can be adopted for the theoretical prediction of tensile and microhardness for different joining processes.

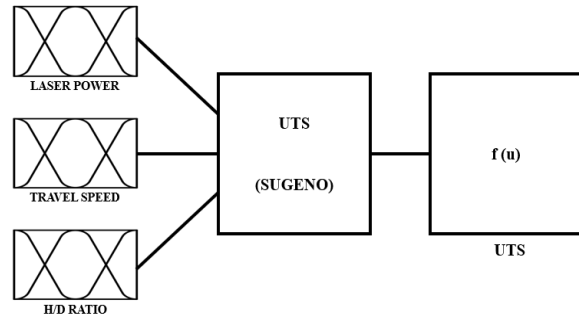


Figure 4. ANFIS model

For each model, 45 data pairs of actual experimental outputs and ANFIS projected outputs were produced using the leave-one-out cross-validation approach. The formula used for obtaining the predicted ANFIS values is given in (1).

$$\text{Predicted Anfis TS} = \text{evalfis}(\text{UTS}, \text{Output}); \quad (1)$$

In a fuzzy set theory, the membership function defines the degree of truth which will be positioned between 0 and 1. This greatly helps to solve undefined problems easily. Generally, the membership functions are represented as curve-like shapes where each curve is termed with different terminology (trimpf, pimf, gbellmf, gaussmf, and gauss2mf). Table 4 refers to the RMSE and MAPE (%) values for each membership function that is arrived at for the UTS plot performed in this work. The least values of RMSE and MAPE (%) are found to be a more reliable membership function to be adopted for the development of the ANFIS model. The least values of RMSE and MAPE (%) in a membership function will be providing the mere values of UTS when compared with the experimentally arrived (UTS) values. The other membership functions also provide the predicted values, but they can be neglected due to their large variations and errors when compared with the actual experimental values. Table 7 shows the comparison between the actual microhardness values with their predicted values arrived with the ANFIS model.

For each model, 45 data pairs of actual experimental outputs and ANFIS projected outputs were produced using the leave-one-out cross-validation approach. The formula used for obtaining the predicted ANFIS values is given in (2):

$$\text{Predicted Anfis Hv} = \text{evalfis}(\text{Hv}, \text{Output}); \quad (2)$$

**Table 4. Membership function**

Number of 'mf'			Type of Membership Function	RMSE (MPa)	MAPE (%)
Laser Power	Travel Speed	UTS			
3	3	2	trimf	52.3782	17.6428
2	3	3	pimf	45.1246	23.1395
3	2	2	pimf	52.3743	18.1266
5	5	3	pimf	42.8417	17.6892
2	3	2	gbellmf	57.8861	15.1977
2	2	3	gaussmf	39.0936	13.0598
5	5	2	gauss2mf	49.7295	15.8533

**Table 5. Comparison of ANFIS predicted UTS vs the Actual Experimental UTS values with Error.**

Laser power (W)	Travel speed (mm/s)	Drill hole depth (mm)	Experimental UTS (MPa)	Predicted Anfis UTS (MPa)	Error %
180	5	3	540	540.167	0.167
181	5	4	550	549.515	-0.485
182	5	5	554	554.413	0.413
183	5	3	557	557.034	0.034
184	5	4	560	559.731	-0.269
185	5	5	563	563.140	0.140
186	5	3	566	566.098	0.098
187	5	4	569	568.894	-0.106
188	5	5	572	571.955	-0.045
189	5	3	575	575.048	0.048
190	5	4	578	578.005	0.005
180	6	5	532	532.616	0.616
181	6	3	535	534.114	-0.886
182	6	4	538	537.551	-0.449
183	6	5	544	545.720	1.720
184	6	3	558	556.399	-1.601
185	6	4	563	563.392	0.392
186	6	5	566	566.569	0.569
187	6	3	569	568.654	-0.346
188	6	4	572	571.726	-0.274
189	6	5	575	575.361	0.361
190	6	3	578	577.900	-0.100
180	7	4	532	531.949	-0.051
181	7	5	535	535.231	0.231
182	7	3	538	537.555	-0.445
183	7	4	541	541.349	0.349
184	7	5	544	544.248	0.248
185	7	3	547	545.983	-1.017
186	7	4	551	552.292	1.292
187	7	5	564	563.264	-0.736
188	7	3	572	571.807	-0.193
189	7	4	575	575.584	0.584
190	7	5	578	577.734	-0.266
180	8	3	532	531.227	-0.773
181	8	4	535	536.508	1.508
182	8	5	538	538.460	0.460
183	8	3	541	540.211	-0.789
184	8	4	544	543.246	-0.754
185	8	5	547	547.957	0.957
186	8	3	550	550.537	0.537
187	8	4	553	552.535	-0.465
188	8	5	556	556.396	0.396
189	8	3	559	558.382	-0.618
190	8	4	568	568.431	0.431

**Table 6. Membership function**

Number of 'mf'			Type of Membership Function	RMSE (Hv)	MAPE (%)
Laser Power	Travel Speed	Microhardness			
3	3	2	trimf	45.5572	18.8656
2	3	3	pimf	52.6912	15.1258
3	2	2	pimf	38.0177	14.2795
5	5	3	pimf	58.8656	16.5684

2	3	2	gbellmf	47.0655	17.0167
2	2	3	gaussmf	37.0395	13.0663
5	5	2	gauss2mf	54.5618	14.0355

**Table 7. Comparison of ANFIS predicted Microhardness vs the Actual Experimental Microhardness values with Error.**

Laser power (W)	Travel speed (mm/s)	Drill hole depth (mm)	Experimental Microhardness (Hv)	Predicted Anfis Microhardness (Hv)	Error %
180	5	3	234	234.498	0.498
181	5	4	256	254.575	-1.425
182	5	5	259	260.495	1.495
183	5	3	261	260.443	-0.557
184	5	4	262	261.789	-0.211
185	5	5	264	264.206	0.206
186	5	3	265	265.310	0.310
187	5	4	267	266.420	-0.580
188	5	5	268	268.326	0.326
189	5	3	270	270.016	0.016
190	5	4	271	270.925	-0.075
180	6	5	221	220.919	-0.081
181	6	3	222	222.410	0.410
182	6	4	224	223.215	-0.785
183	6	5	232	232.826	0.826
184	6	3	258	257.146	-0.854
185	6	4	264	264.934	0.934
186	6	5	265	264.729	-0.271
187	6	3	267	266.328	-0.672
188	6	4	268	268.658	0.658
189	6	5	270	269.852	-0.148
190	6	3	271	270.983	-0.017
180	7	4	221	221.130	0.130
181	7	5	222	221.616	-0.384
182	7	3	223	223.169	0.169
183	7	4	225	225.122	0.122
184	7	5	226	226.421	0.421
185	7	3	227	226.113	-0.887
186	7	4	232	232.762	0.762
187	7	5	256	255.464	-0.536
188	7	3	268	267.788	-0.212
189	7	4	270	270.867	0.867
190	7	5	271	270.547	-0.453
180	8	3	221	220.483	-0.517
181	8	4	222	222.365	0.365
182	8	5	223	222.175	-0.825
183	8	3	225	225.594	0.594
184	8	4	226	225.523	-0.477
185	8	5	227	227.368	0.368
186	8	3	228	227.390	-0.610
187	8	4	230	229.199	-0.801
188	8	5	231	231.539	0.539
189	8	3	233	232.108	-0.892
190	8	4	249	249.507	0.507

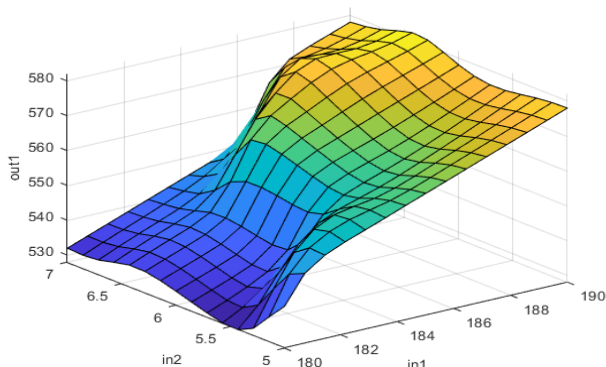


**Figure 5. Surface plot for UTS varying laser power and travel speed.**

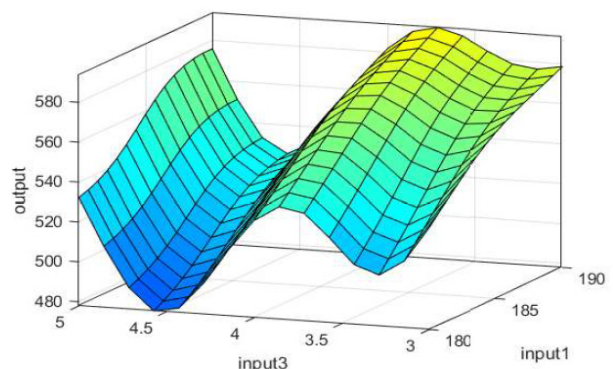


**Figure 6. Surface plot for UTS varying laser power and hole depth ratio.**

The Surface plot helps visualize the welding process parameters necessary to obtain specific tensile strength values. The Surface plot is plotted in Figures 5 and 6. Figure 5 illustrates Laser Power on the X-axis, Travel Speed on the Y-axis, and the UTS value is plotted on the Z-axis, while Figure 6 describes Laser Power on the X-axis, Hole Depth Ratio on the Y-axis, and the UTS value is plotted on the Z-axis.

### 5. UCNN MODELLING AND VALIDATION

UCNN tool is a novel method for predicting defects in the welded samples through the image processing technique. The test trials are performed with the application of MATLAB software and the accuracy values are listed in table 8. The fabricated joints of laser and TIG welding samples are observed in the optical microscope for their metallurgical behavior. The optical survey is focused on the fusion zone and heat-affected zone to understand the solidification of the metal. Fig. 3 (C & D) depicts the fusion zone metallurgical behavior of two different welding processes. Among these two, figure 3(C) has been imported into the MATLAB portal for the prediction of the defects shown in Figure 7. Figure 8 shows the accuracy validation plot obtained from the MATLAB portal for the respective image.

It can be observed in Table 8 that the accuracy value is higher for laser-welded when compared with the TIG welded sample. A higher accuracy value proves the defect in the respective sample is at the lower end when compared with the other samples. Figures 9, 10, & 11 represent the various plots obtained for the different medians that are utilized in the image processing technique and it can be depicted from the figures that the accuracy values are

higher for samples that are low in the mean square error, high (PSNR) value, and low in the processing time.

Clustered Image using 2D-ACEM

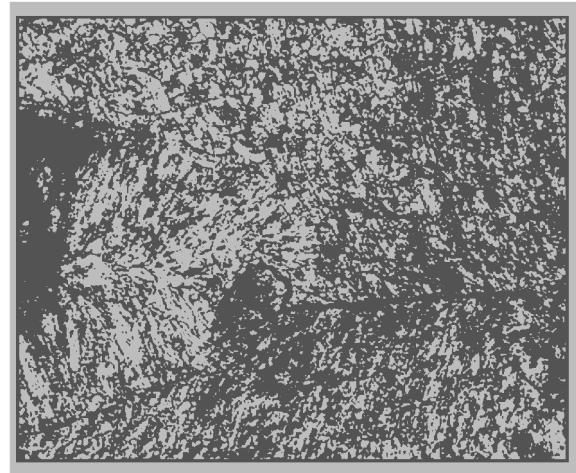


Figure 7. Optical image of FZ laser-welded sample.

The accuracy values obtained for the samples show a good agreement with the experimental test result values. Thus, the UCNN tool can be adopted to predict defects in the weldment instead of existing traditional methods.

Table 8. Accuracy validation plot for the optical images obtained in different zones.

SI. No	Zones & weld process	Accuracy value from MATLAB
1	FZ – TIG	91.64
2	HAZ – TIG	92.62
3	FZ – LW	94.96
4	HAZ – LW	94.20

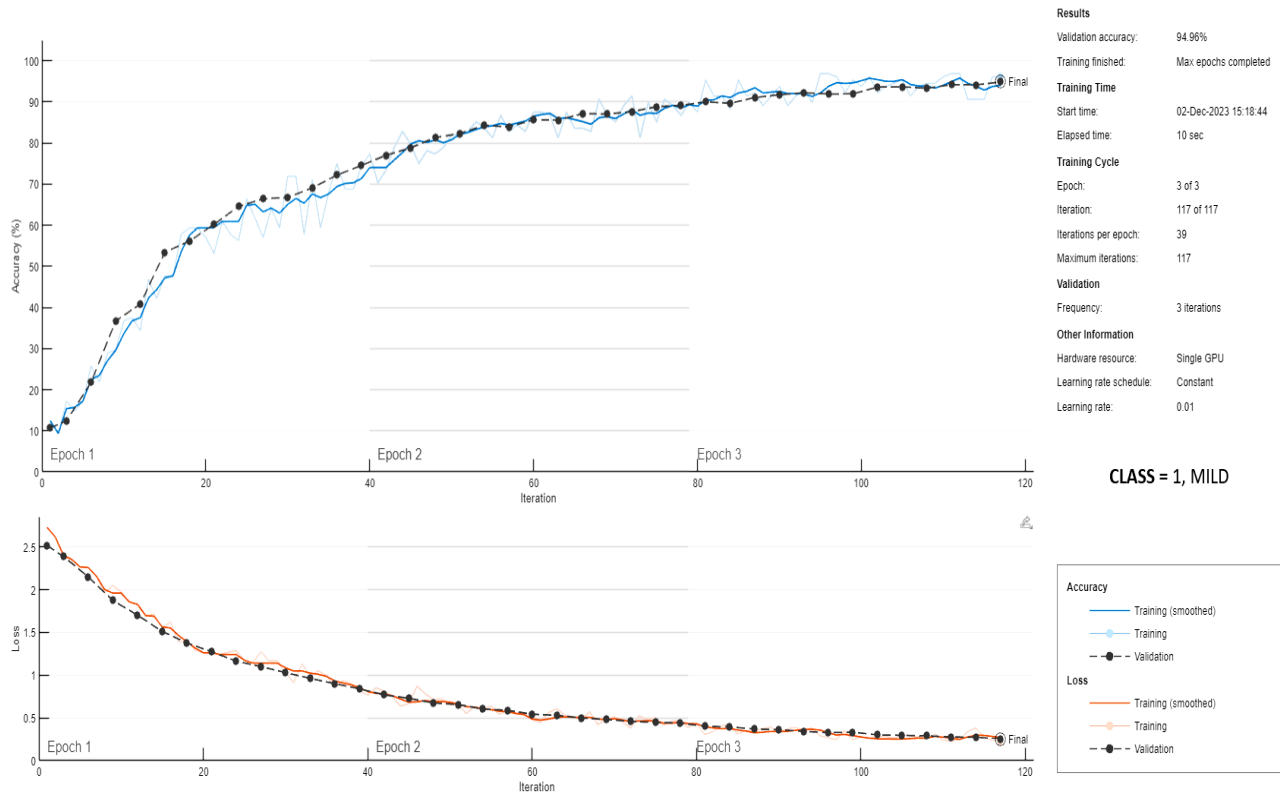


Figure 8. Accuracy validation plot.

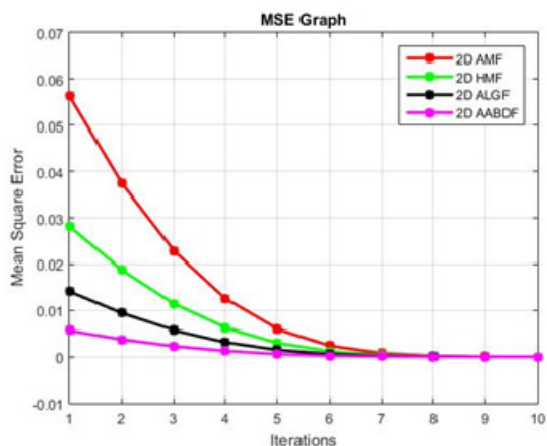


Figure 9. Mean square error plot from MATLAB using different algorithms.

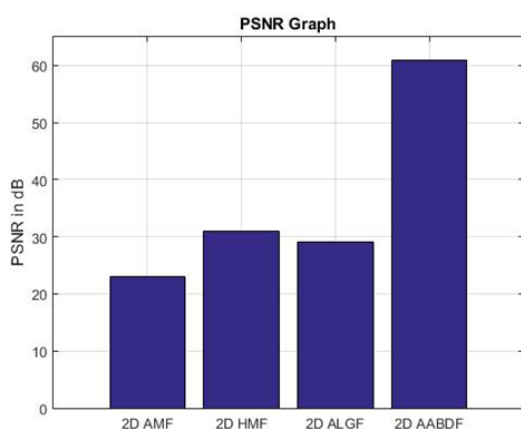


Figure 10. PSNR graph plot for different algorithms.

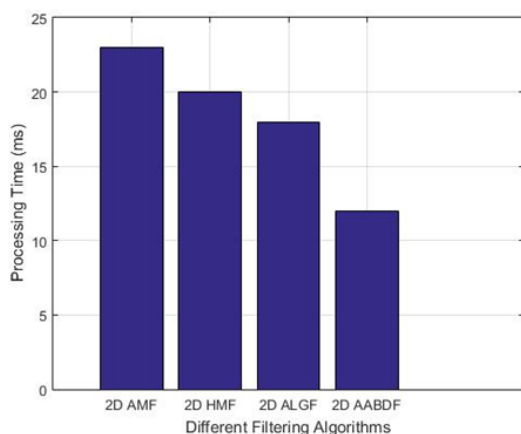


Figure 11. Processing time plots for different algorithms.

## 6. EVALUATION OF ANFIS & UCNN MODELS

From the obtained results it is found that the predicted mechanical properties (tensile strength and microhardness) of the ANFIS model are in good agreement with the experimental results. Similarly, the UCNN tool using different adaptive filters resulted in higher (PSNR) and Least Mean Square Error (MSE) values for the sample fabricated with the laser welding process which is also found to be in good understanding with the obtained metallographic results. From the inferred results of the machine learning techniques, the laser-welded sample has shown promising results in the

image processing technique. It is reported in our previous study [47], that the refinement of grain boundaries is achieved with the addition of powders with the base metal. Moreover, the ( $\delta$ -Fe) content also had a significant effect on the metallurgical properties of the weldments. However, these enhancements in the metallurgical property of the metal are also due to the joining process that we adopt for the fabrication. In this situation, laser welding had made a good effect on the enhancement of metallurgical characteristics of the weldment when compared with the TIG welded sample. The improvement in the metallurgical aspects of the sample had a promising effect on the PSNR and MSE values obtained through the image processing technique. Thus, both machine learning approaches are sound enough for the welding process to determine either the numerical values or those related to defect prediction.

## 7. CONCLUSION

The present investigation has demonstrated two different machine learning approaches, one approach pertaining to the prediction of tensile and microhardness values, and the other one is the prediction of defects from the optical images obtained from the samples. This study will provide a comparison of the two different machine-learning approaches. In addition to this, the adoption of these machine learning techniques could be more reliable for the better optimization of the process parameters. The drawn conclusions from this study are reported below.

1. ANFIS model analysis was performed based on the Takagi-Sugeno approach.

2. The UCNN model was developed with the assistance of 4 different filters (Adaptive Median Filter, 2D Hybrid Median Filter, 2D Adaptive Log Gabor, 2D Adaptive Anisotropic Bilateral Diffusion Filter).

3. The ANFIS model is developed to predict the tensile and microhardness values. The UCNN model is developed for the prediction of defects in the weldment through image processing techniques.

4. The two different machine learning approaches adopted in this study had good agreement with the obtained experimental test results.

5. The predicted values of the ANFIS model for the laser-welded sample are well accommodated with the (PSNR) value obtained from the image processing technique for a similar laser-welded sample. Therefore, these two different techniques can be widely utilized for the prediction of values or defects.

6. However, the (PSNR) values are found to be less for the TIG welded sample, this variation in the (PSNR) values is due to the different welding processes. Thus, the optimal selection of the welding process is also observed to be highly influential in the metallurgical aspects.

7. It is found that the MSE value is minimal in both the developed models, the (2D Adaptive Anisotropic Bilateral Diffusion Filter) of the UCNN showed the least value among the other filters adopted.

8. However, the adoption of the ANFIS model has had a significant effect on the selection of process parameters. Based on this model with the assumed

process parameters, we could be able to identify the predicted mechanical property values with ease. Thus, it reduces the difficulty that occurs in the conventional optimization of process parameters which requires more trial and error methodologies.

9. The utilization of the UCNN model is reliable in predicting the defects in the fabricated sample without much complexity, that occur in the conventional NDT techniques. The conventional NDT methods require more pre and post-processing approach which also takes much amount of time. Whereas, with the adoption of the UCNN model it is easy to overcome those issues.

10. Thus, both machine learning techniques can be adopted in the welding process. Concerning the application requirement, we need to use the appropriate machine-learning techniques.

### CONFLICT OF INTEREST

The authors declare that there is no conflict of interest.

### REFERENCES

- [1] Lee, H.T., Jeng, S.L.: Characteristics of dissimilar welding of alloy 690 to 304L stainless steel. *Sci. Technol. Weld. Join.* 6, 225–234 (2001). <https://doi.org/10.1179/136217101101538811>
- [2] Jamshidi Aval, et al.: Theoretical and experimental study of microstructures and weld pool geometry during GTAW of 304 stainless steels. *Int. J. Adv. Manuf. Technol.* 42, 1043–1051 (2009). <https://doi.org/10.1007/s00170-008-1663-6>
- [3] Li, Z., Gobbi, S.L., Richter, K.H.: Autogenous welding of Hastelloy X to Mar-M 247 by laser. *J. Mater. Process. Technol.* 70, 285–292 (1997). [https://doi.org/10.1016/S0924-0136\(97\)02939-7](https://doi.org/10.1016/S0924-0136(97)02939-7)
- [4] Sun, Z., Kuo, M.: Bridging the joint gap with wire feed laser welding. *J. Mater. Process. Technol.* 87, 213–222 (1999). [https://doi.org/10.1016/S0924-0136\(98\)00346-X](https://doi.org/10.1016/S0924-0136(98)00346-X)
- [5] Junaid, M., Rahman, K., Khan, F.N., Bakhsh, N., Baig, M.N.: Comparison of microstructure, mechanical properties, and residual stresses in tungsten inert gas, laser, and electron beam welding of Ti–5Al–2.5Sn titanium alloy. *Proc. Inst. Mech. Eng. Part L J. Mater. Des. Appl.* 233, 1336–1351 (2019). <https://doi.org/10.1177/1464420717748345>
- [6] Rajasekaran, R. et al.: Role of welding processes on microstructure and mechanical properties of nuclear grade stainless steel joints. *Proc. Inst. Mech. Eng. Part L J. Mater. Des. Appl.* 233, 2335–2351 (2019). <https://doi.org/10.1177/1464420719849448>
- [7] Yan, J., Gao, M., Zeng, X.: Study on microstructure and mechanical properties of 304 stainless steel joints by TIG, laser and laser-TIG hybrid welding. *Opt. Lasers Eng.* 48, 512–517 (2010). <https://doi.org/10.1016/j.optlaseng.2009.08.009>
- [8] Soltani, H.M., Tayebi, M.: Comparative study of AISI 304L to AISI 316L stainless steels joints by TIG and Nd: YAG laser welding. *J. Alloys Compd.* 767, 112–121 (2018). <https://doi.org/10.1016/j.jallcom.2018.06.302>
- [9] Kumar, N., Mukherjee, M., Bandyopadhyay, A.: Comparative study of pulsed Nd: YAG laser welding of AISI 304 and AISI 316 stainless steels. *Opt. Laser Technol.* 88, 24–39 (2017). <https://doi.org/10.1016/j.optlastec.2016.08.018>
- [10] Chen, S., Zhang, M., Huang, J., Cui, C., Zhang, H., Zhao, X.: Microstructures and mechanical property of laser butt welding of titanium alloy to stainless steel. *Mater. Des.* 53, 504–511 (2014). <https://doi.org/10.1016/j.matdes.2013.07.044>
- [11] Scintilla, L.D., Tricarico, L., Brandizzi, M., Satriano, A.A.: Nd: YAG laser weldability and mechanical properties of AZ31 magnesium alloy butt joints. *J. Mater. Process. Technol.* 210, 2206–2214 (2010). <https://doi.org/10.1016/j.jmatprotec.2010.08.005>
- [12] Khajanchee, A., Pradhan, S.K., Jain, P.: Experimental Investigations to Optimize Process Parameters for CO<sub>2</sub> Laser Welded Alloy Steel Automotive Gears. *Mater. Today Proc.* 5, 11636–11654 (2018). <https://doi.org/10.1016/j.matpr.2018.02.134>
- [13] Huang, Y. et al.: Optimization of weld strength for laser welding of steel to PMMA using Taguchi design method. *Opt. Laser Technol.* 136, 106726 (2021). <https://doi.org/10.1016/j.optlastec.2020.106726>
- [14] Behera, A.: Optimization of process parameters in laser welding of dis-similar materials. *Mater. Today Proc.* 33, 5765–5769 (2020). <https://doi.org/10.1016/j.matpr.2020.07.148>
- [15] Anawa, E.M., Olabi, A.G.: Using Taguchi method to optimize welding pool of dissimilar laser-welded components. *Opt. Laser Technol.* 40, 379–388 (2008). <https://doi.org/10.1016/j.optlastec.2007.07.001>
- [16] Cao, X., Li, Z., Zhou, X., Luo, Z., Duan, J.: Modeling and optimization of resistance spot welded aluminum to Al-Si coated boron steel using response surface methodology and genetic algorithm. *Measurement.* 171, 108766 (2021). <https://doi.org/10.1016/j.measurement.2020.108766>
- [17] Long, J., Huang, W., Xiang, J., Guan, Q., Ma, Z.: Parameter optimization of laser welding of steel to Al with pre-placed metal powders using the Taguchi-response surface method. *Opt. Laser Technol.* 108, 97–106 (2018). <https://doi.org/10.1016/j.optlastec.2018.06.026>
- [18] Benyounis, K.Y., et al.: Multi-response optimization of CO<sub>2</sub> laser-welding process of austenitic stainless steel. *Opt. Laser Technol.* 40, 76–87 (2008). <https://doi.org/10.1016/j.optlastec.2007.03.009>
- [19] Gunaraj, V., Murugan, N.: Application of response surface methodology for predicting weld bead quality in submerged arc welding of pipes. *J. Mater. Process. Technol.* 88, 266–275 (1999). [https://doi.org/10.1016/S0924-0136\(98\)00405-1](https://doi.org/10.1016/S0924-0136(98)00405-1)
- [20] Khan, M.M.A., Romoli, L., Fiaschi, M., Dini, G., Sarri, F.: Experimental design approach to the process parameter optimization for laser welding of martensitic stainless steels in a constrained overlap configuration. *Opt. Laser Technol.* 43, 158–172 (2011). <https://doi.org/10.1016/j.optlastec.2010.06.006>

- [21] Zhang, Y.M., Kovacevic, R., Li, L.: Characterization and real-time measurement of geometrical appearance of the weld pool. *Int. J. Mach. Tools Manuf.* 36, 799–816 (1996). [https://doi.org/10.1016/0890-6955\(95\)00083-6](https://doi.org/10.1016/0890-6955(95)00083-6)
- [22] Kovacevic, R., Zhang, Y., Li, L.: Monitoring of Weld Joint Penetrations Based on Weld Pool Geometrical Appearance: The geometrical appearance of the weld pool contains sufficient information to determine full joint penetration in GTAW, (1996)
- [23] Sathiya, P., Panneerselvam, K., Abdul Jaleel, M.Y.: Optimization of laser welding process parameters for super austenitic stainless steel using artificial neural networks and genetic algorithm. *Mater. Des.* 36, 490–498 (2012). <https://doi.org/10.1016/j.matdes.2011.11.028>
- [24] Park, Y.W., Rhee, S.: Process modeling and parameter optimization using neural network and genetic algorithms for aluminum laser welding automation. *Int. J. Adv. Manuf. Technol.* 37, 1014–1021 (2008). <https://doi.org/10.1007/s00170-007-1039-3>
- [25] Liu, Y., Zhang, Y.: Iterative Local ANFIS-Based Human Welder Intelligence Modeling and Control in Pipe GTAW Process: A Data-Driven Approach. *IEEE/ASME Trans. Mechatronics.* 20, 1079–1088 (2015). <https://doi.org/10.1109/TMECH.2014.2363050>
- [26] Correia, D.S., Gonçalves, C.V., da Cunha, S.S., Ferraresi, V.A.: Comparison between genetic algorithms and response surface methodology in GMAW welding optimization. *J. Mater. Process. Technol.* 160, 70–76 (2005). <https://doi.org/10.1016/j.jmatprotec.2004.04.243>
- [27] Juang, S., Tarn, Y.: Process parameter selection for optimizing the weld pool geometry in the tungsten inert gas welding of stainless steel. *J. Mater. Process. Technol.* 122, 33–37 (2002). [https://doi.org/10.1016/S0924-0136\(02\)00021-3](https://doi.org/10.1016/S0924-0136(02)00021-3)
- [28] Katherasan, D., Elias, J. V., Sathiya, P., Haq, A.N.: Simulation and parameter optimization of flux cored arc welding using artificial neural network and particle swarm optimization algorithm. *J. Intell. Manuf.* 25, 67–76 (2014). <https://doi.org/10.1007/s10845-012-0675-0>
- [29] Ai, Y., Shao, X., Jiang, P., Li, P., Liu, Y., Liu, W.: Welded joints integrity analysis and optimization for fiber laser welding of dissimilar materials. *Opt. Lasers Eng.* 86, 62–74 (2016). <https://doi.org/10.1016/j.optlaseng.2016.05.011>
- [30] Ma, X. et al.: Optimization of the welding process parameters of Mg–5Gd–3Y magnesium alloy plates with a hybrid Kriging and particle swarm optimization algorithm. *Proc. Inst. Mech. Eng. Part C J. Mech. Eng. Sci.* 232, 4038–4048 (2018). <https://doi.org/10.1177/0954406217747911>
- [31] Jang, J.-S.R.: ANFIS: adaptive-network-based fuzzy inference system. *IEEE Trans. Syst. Man. Cybern.* 23, 665–685 (1993). <https://doi.org/10.1109/21.256541>
- [32] Dewan, M.W., Huggett, D.J., Warren Liao, T., Wahab, M.A., Okeil, A.M.: Prediction of tensile strength of friction stir weld joints with adaptive neuro-fuzzy inference system (ANFIS) and neural network. *Mater. Des.* 92, 288–299 (2016). <https://doi.org/10.1016/j.matdes.2015.12.005>
- [33] Zaharuddin, M.F.A., Kim, D., Rhee, S.: An ANFIS based approach for predicting the weld strength of resistance spot welding in artificial intelligence development. *J. Mech. Sci. Technol.* 31, 5467–5476 (2017). <https://doi.org/10.1007/s12206-017-1041-0>
- [34] Yilmaz, N.F., Kurt, H.I., Oduncuoglu, M., Ergul, E.: Experimental and theoretical analysis of the welding process parameters for UTS with different methods. *Mater. Res. Express.* 6, 016524 (2018). <https://doi.org/10.1088/2053-1591/aae348>
- [35] Okafor, C.E., Okafor, E.J., Ikebudu, K.O.: Evaluation of machine learning methods in predicting optimum tensile strength of microwave post-cured composite tailored for weight-sensitive applications. *Eng. Sci. Technol. an Int. J.* 25, 100985 (2022). <https://doi.org/10.1016/j.jestch.2021.04.004>
- [36] Chen, C., Xiao, R., Chen, H., Lv, N., Chen, S.: Prediction of welding quality characteristics during pulsed GTAW process of aluminum alloy by multisensory fusion and hybrid network model. *J. Manuf. Process.* 68, 209–224 (2021). <https://doi.org/10.1016/j.jmapro.2020.08.028>
- [37] Zhang, Y., You, D., Gao, X., Zhang, N., Gao, P.P.: Welding defects detection based on deep learning with multiple optical sensors during disk laser welding of thick plates. *J. Manuf. Syst.* 51, 87–94 (2019). <https://doi.org/10.1016/j.jmsy.2019.02.004>
- [38] Zhang, B., Hong, K.-M., Shin, Y.C.: Deep-learning-based porosity monitoring of laser welding process. *Manuf. Lett.* 23, 62–66 (2020). <https://doi.org/10.1016/j.mfglet.2020.01.001>
- [39] Bacioiu, D., Melton, G., Papaalias, M., Shaw, R.: Automated defect classification of SS304 TIG welding process using visible spectrum camera and machine learning. *NDT E Int.* 107, 102139 (2019). <https://doi.org/10.1016/j.ndteint.2019.102139>
- [40] Park, J.-K., An, W.-H., Kang, D.-J.: Convolutional Neural Network Based Surface Inspection System for Non-patterned Welding Defects. *Int. J. Precis. Eng. Manuf.* 20, 363–374 (2019). <https://doi.org/10.1007/s12541-019-00074-4>
- [41] Malaravel, M., Sethumadhavan, G., Rao Bhagi, P.C., Kar, S., Saravanan, T., Krishnan, A.: Anisotropic diffusion based denoising on X-radiography images to detect weld defects. *Digit. Signal Process.* 68, 112–126 (2017). <https://doi.org/10.1016/j.dsp.2017.05.014>
- [42] Zahran, O., Kasban, H., El-Kordy, M., El-Samie, F.E.A.: Automatic weld defect identification from

- radiographic images. *NDT E Int.* 57, 26–35 (2013). <https://doi.org/10.1016/j.ndteint.2012.11.005>
- [43] Halim, S.A., Ibrahim, A., Manurung, Y.H.P.: Digital radiographic image enhancement for weld defect detection using smoothing and morphological transformations. *Sci. Res. J.* 9, 15–28 (2012)
- [44] Kountchev, R.K., Rubin, S.H., Todorov, V.T., Kountcheva, R.A.: Automatic detection of welding defects. *Int. J. Reason. Intell. Syst.* 3, 34–43 (2011). <https://doi.org/10.1504/IJRIS.2011.037739>
- [45] Cheng, Y., Deng, H., Feng, Y., Xiang, J.: Weld Defect Detection and Image Defect Recognition using Deep Learning Technology. 1–7 (2021). <https://doi.org/10.21203/rs.3.rs-149365/v1>
- [46] J. Kadhim, S., K. Al-Sabur, R., K. Ali, A.B.: Application of Different Median Filter Algorithms for Welding Defects Clarification in Radiographic Images. *Univ. Thi-Qar J. Eng. Sci.* 11.1, 56–61 (2020). <https://doi.org/10.31663/tqujes.11.1.378> (2020).
- [47] Varun Kumar, A., Selvakumar, A.S., Balachandrar, K., Waseem Ahmed, A., Yashar Arabath, A.: Correlation between material properties and free vibration characteristics of TIG and laser welded stainless steel 304 reinforced with Al<sub>2</sub>O<sub>3</sub> micro-particles. *Eng. Sci. Technol. an Int. J.* 24, 1253-1261 (2021). <https://doi.org/10.1016/j.jestch.2021.01.017>.
- [48] Gemici, E. et al.: Predicting Cone Production in Clonal Seed Orchard of Anatolian Black Pine with Artificial Neural Network. *Appl. Ecol. Environ. Res.* 17, 2267–2273 (2019). [https://doi.org/10.15666/aeer/1702\\_22672273](https://doi.org/10.15666/aeer/1702_22672273).
- [49] Andersen, K., Cook, G.E., Karsai, G., Ramaswamy, K.: Artificial neural networks applied to arc welding process modeling and control. *IEEE Trans. Ind. Appl.* 26, 824–830 (1990). <https://doi.org/10.1109/28.60056>.
- [50] Yuguang, Z., Kai, X., Dongyan, S.: An improved artificial neural network for laser welding parameter selection and prediction. *Int. J. Adv. Manuf. Technol.* 68, 755–762 (2013). <https://doi.org/10.1007/s00170-013-4796-1>.
- [51] Sujit G., Sudipto C.: Estimation and optimization of depth of penetration in hybrid CO<sub>2</sub> LASER-MIG welding Using ANN-optimization hybrid model, *Int. J. Adv. Manuf. Technol.* 47, 1149-1157 (2010). DOI 10.1007/s00170-009-2234-1.
- [52] A. Sanchez Roca, H. C. Fals, J. B. Fernandez, E. J. Macias and M. P. de la Parte, Artificial neural networks and acoustic emission applied to stability analysis in gas metal arc welding, *Science and Technology of Welding and Joining*, 14, 2009.
- [53] Ming-Jong Tsai, Chen-Hao Li, Cheng-Che Chen, Optimal laser-cutting parameters for QFN packages by utilizing artificial neural networks and genetic algorithm, 208, 270-283, 2008. doi:10.1016/j.jmatprotec.2007.12.138.
- [54] Nada R. Ratković, Dušan M. Arsić, Vukić N. Lazić, Ružica R. Nikolić, Branislav Hadzima, Peter Palček, Aleksandar S. Sedmak, Influence of Friction Welding Parameters on Properties of the Al-Cu Joint, *FME Transactions* (2017) 45, 165-171.
- [55] Anna O. Lukinenko, Sviatoslav I. Motrunich, Darko Bajić, Vasily A. Kuleshov, Anatolii G. Pokliatskyi, Tetiana M. Labur, Noise Level Assessment and Mechanical Properties of Welded Joints of Aluminium Alloys of the Al-Cu-Li System in FSW and TIG Welding, *FME Transactions* (2021) 49, 220-224.
- [56] Anna Lukianenko, Tetiana M. Labur, Anatolii G. Pokliatskyi, Sviatoslav Motrunich, Darko Bajić, Investigation of Fatigue Strength and Norms of Emission of Harmful Substances in the Air during MIG and TIG Welding of 1460 Aluminium-Lithium Alloy, *FME Transactions* (2019) 47, 608-612.
- [57] Miroslava Ťavodová, Nataša Náprstková, Michaela Hnilicová, Pavel Beňo, Quality Evaluation of Welding Joints by Different Methods, *FME Transactions* (2020) 48, 816-824.
- [58] Harinadh Vemaaboina, Suresh Akella, Ramesh Kumar Buddu, Distortion Control in Laser Beam Welding using Taguchi ANOVA Analysis, *FME Transactions* (2020) 48, 180-186.

#### Nomenclature

W	Watt
A	Amps
Hv	Microhardness
Mf	Membership function

#### Acronyms

Nd YAG	Neodymium Yttrium Aluminum Garnet
TIG	Tungsten Inert Gas Welding
Hv	Microhardness
ANFIS	Artificial Neuro-Fuzzy Interface System
UCNN	Unified Convolutional Neural Network
ASS	Austenitic Stainless Steel
LBW	Laser Beam Welding
GTAW	Gas Tungsten Arc Welding
HAZ	Heat Affected Zone
ANN	Artificial Neural Network
ANOVA	Analysis of Variance
PSNR	Peak Signal to Noise Ratio
AMF	Adaptive Median Filter
NDT	Non-Destructive Testing
RMSE	Root Mean Square Error
MAPE	Mean Absolute Percentage Error
UTS	Ultimate Tensile Strength

#### ОЦЕНА ТЕХНИКА МАШИНСКОГ УЧЕЊА ЗА НД: ИАГ ЛАСЕР И ТИГ ЗАВАРЕНИ НЕРЉАЈУЊИ ЧЕЛИК 304

А.В. Кумар, Р.П. Кришна, Х.М. Фақури,  
К. Сачикбаша

Процеси заваривања Нд: ИАГ ласером и инертним гасом од волфрама (ТИГ) су најперспективније

технике спајања које се користе за легуре нерђајућег челика (СС) због њихових значајних карактеристика заvara. У овој студији истражује се утицај два параметра процеса (снага заvara и брзина кретања) на механичка својства (крајња затезна чврстоћа и микротврдоћа) завареног споја. Две различите технике машинског учења, а то су Адаптиве Неуро-Фуззи Инференце Систем (АНФИС) и Унифид Цонволуционал Неурал Нетворк (УЦНН), такође се процењују за предвиђање механичких својстава и детекцију дефеката кроз технику обраде слике, респективно. Извршена је корелација између ова два приступа машинском учењу са експерименталним вредностима. Скупови података за обуку су разви-

јени за технике машинског учења, а добијени резултати (АНФИС) и (УЦНН) модела су повезани са стварним експерименталним вредностима. Резултат оба развијена модела (АНФИС & УЦНН) показао је добро слагање са стварним експерименталним резултатима теста. Утврђено је да се предвиђене вредности затезања и микротврдоће из (АНФИС) модела у великој мери слажу са вредностима вршног односа сигнал-шум (ПСНР) из (УЦНН) модела. Међутим, захваљујући повећању примене процеса заваривања у индустрији, коришћење техника машинског учења било би ефикасније у поређењу са другим традиционалним методама које се усвајају.